Supporting Information

Transforming Complexity to Simplicity: Protein-like Nanotransformer for Improving Tumor Drug Delivery Programmatically

*Hui Xiong[a], Zihan Wang[a], Cheng Wang[b], Jing Yao[a]**

[a]State Key Laboratory of Natural Medicines and Jiangsu Key Laboratory of Druggability of Biopharmaceuticals, Department of Pharmaceutics, China Pharmaceutical University, 639 Longmian Avenue, Nanjing 211198, China

[b]School of Food Science and Pharmaceutical Engineering, Nanjing Normal University, No. 1 Wenyuan Road, Nanjing, 210046, China

* Correspondence to: Jing Yao, E-mail: yaojing@cpu.edu.cn

KEYWORDS: Hydrophilic-hydrophobic conversion, nanoparticles with alterable size, proton-responsiveness, combination therapy, self-assembled nanoparticles

Supporting Methods

Materials. Doxorubicin (DOX) was acquired from Nanjing Shengli De Biotech Co., Ltd. (Nanjing, China); Tannin (TA) was from Aladdin Reagent (Shanghai) Co., Ltd.;Indocyanine green (ICG) was provided by Sam Chemical Technology Co., Ltd.

(Shanghai, China); 4,6-diamidino-2-phenylindole (DAPI), Cell Counting Kit-8 (CCK-8) were all from Beyotime Inc. (Shanghai, China). All other chemicals and reagents were from Sinopharm Chemical reagent Co., LTD and of analytical grade.

*Cell culture:*MCF7 cells were cultured in dulbecco's modified eagle medium (DMEM) with 10% (v/v) fetal bovine serum (Zhejiang Tianhang Biological technology stock Co., Ltd., China) and 100 units mL^{-1} penicillin &100 μg mL^{-1} streptomycin solution in an atmosphere of 95% air and 5% CO_2 at 37℃. Logarithmic cells were used in all experiments.

Multicellular tumor spheres (MTS): 96-well plate was coated with 50 μL per well high-pressure sterilized agarose solution (1.5%, w/v), then cooled to room temperature. MCF7 cells were put in the plate at the density of 3×10^3 cells per pore and cultured at incubator for 3-4 days. Tumor morphology was observed.

Animal model: Female nude mice were supplied by Shanghai Laboratory Animal Center (SLAC, China). All the mice were lived in a temperature controlled environment (25℃) with free access to water and food. All experiments were approved by the Animal Center Laboratory of Zhejiang University. The suspension of MCF7 cells were inoculated subcutaneously in the flank of nude mice. The volumes of tumors were calculated as $V = a^2\times b/2$ mm^3 (a: minor axis of tumor; b: major axis of tumors).

Preparation and characterization of DTIG. DTIG were prepared by DOX•HCl, TA and ICG. All reagents were dissolved in a proper amount of water. Firstly, DOX and TA were assembled by stirring for 5 min. Then, 5 mL water was added into this mixture, followed by continuously stirring for another 5 min. After that, ICG was diluted by water and added to the above mixture to stir for 40 min at an appropriate rate (1500 rpm min^{-1}). Subsequently, the mixture was centrifuged at 5000 rpm (10 min) and 10000 rpm (10 min)

continuously. The supernatant was collected for drug loading (DL) measurement and the precipitation was redissolved with 5 mL water and ultrasound for 8 min. The DL was calculated as below: DL = (∆m) / (∆m + m_I+ m_{II}) × 100% (∆m: the difference between the initial weight of DOX or ICG and the DOX or ICG weight in the supernatant; m_I : the weight of TA; m_{II} : the weight of ICG or DOX). The amount of DOX and ICG were tested by UV-vis patterns (TU-1810PC spectrophotometer, PERCEE, China).

The particle size and zeta potential of DTIG were measured by dynamic light scattering (DLS) using Zeta potential and particle size analyzer (NanoBrook Omni, Brookhaven , USA). FTIR (Tensor 27, Bruker Co., Ltd., Germany), Fluorescence Spectroscopy (RF-5301PC, SHIMADZU, Japan), Differential Scanning Calorimeter (DSC, DSC 204 F1 Phoenix®, NETZSCH, Germany), X-ray Diffraction (XRD, D8 Advance, Bruker, German), TEM (HT7700, HITACHI, Japan) and AFM (MultiMode 8, Veeco, America) were used for characterizations of DTIG.

Molecular dynamics simulations analysis. The structures of small molecules DOX, TA and ICG were optimized under B3LYP/6-31G* by Gaussian09[1] package. After that, the HF/6-31G* method and basis set were used to calculate the electrostatic potential (ESP) and then the result was employed to calculate the restricted ESP(RESP)[2] charge. MMFF94x[3] Force Field parameters were used for small molecules. First of all, 16 molecules DOX and 9 molecules TA were initially packed randomly by PACKMOL[4] in a cubic box with the length 80 Å. Then the mixture was neutralized in a cuboid box of TIP3P[5] water molecules with solvent layers 10 Å between the box edges and solute surface.

All molecular dynamics (MDs) simulations were performed using AMBER16[6]. The AMBER GAFF[7] force fields were applied and the SHAKE algorithm was used to restrict

all covalent bonds involving hydrogen atoms with a time step of 2 fs. The Particle Mesh Ewald (PME) method was employed to treat long-range electrostatic interactions. For each solvated system, two steps of minimization were performed before the heating step. The first 4000 cycles of minimization were performed with all heavy atoms restrained with 50 kcal/(mol·Å2), whereas solvent molecules and hydrogen atoms were free to move. Then, non-restrained minimization was carried out involving 2,000 cycles of steepest descent minimization and 2,000 cycles of conjugated gradient minimization. Afterwards, the whole system was first heated from 0 K to 300 K in 50 ps using Langevin dynamics at a constant volume and, then, equilibrated for 400 ps at a constant pressure of 1 atm. A weak constraint of 10 kcal/ (mol·Å2) was used to restrain all the heavy atoms during the heating steps. Periodic boundary dynamics simulations were carried out for the whole system with constant composition, pressure, and temperature ensemble at a constant pressure of 1 atm and 300 K in the production step. In production phase, 50 ns simulation was carried out.

The final stable assembled intermediate product DT was further assembled with ICG. 18 molecules ICG were packed around the product DT randomly by PACKMOL. Then the mixture was neutralized in a cuboid box of TIP3P [5] water molecules with solvent layers 10 Å between the box edges and solute surface. 50 ns simulation same to the above procedure was carried out.

Photothermal performance. 1 mL DTIG was placed in a 5 mL tube and irradiated at the conditions of 808 nm laser and power density of 0.5 W cm^{-2}. The solution temperature was measured by infrared imaging device (FLIR E40 of FLIR Systems, Inc., USA) for 10 min totally. For *in vivo* study, the infrared thermographic maps of MCF7 tumor bearing mice

was captured after injection with DTIG, free ICG, or PBS at 5 min after laser irradiation(1 W cm^{-2}).

Drug release study. *In vitro* drug release study of DTIG was determined using dialysis method. 2 mL DTIG (containing 2 mg DOX and 3 mg ICG) was firstly added into the dialysis bags (MWCO, 3.5 kDa) which were then submerged into 100 mL PBS with different pH. The drug release experiments were performed with and without 1.6 W cm^{-2} 808 nm laser irradiation for 5 min. At predetermined time points, the dissolution media was taken out for test. The cytoplasm of MCF7 was collected as improved reported method.[8] MCF7 cells were firstly disrupted by Ultrasonic Cell Disruption System (Beidi-IIYJ, China) and then the cytoplasm of which were obtained by gradient centrifugation.

Cellular uptake and intercellular drug delivery assay. The uptake of DTIG by tumor cells and the distribution of DTIG in cells were observed by confocal laser scanning microscope (CLSM) (BX61W1-FV1000, Olympus and TE2000-S, Nikon, Japan). 3×10^5 cells per dish MCF7 cells were put in the confocal dishes. After the cells were attached for 12 h, the old medium was discarded and replaced with fresh medium (pH 7.4 or pH 6.5) containing DTIG (5 μg mL^{-1} DOX) or LIBOd® (5 μg mL^{-1} DOX). After incubation for 2 h, cells were fixed by 4% paraformaldehyde, stained with 100 ng mL^{-1} DAPI for 15 min, and washed 3 times with fresh PBS. Meanwhile, Flow Cytometric Analysis (BD, USA) was employed to detect the cellular uptake of DTIG and LIBOd® in different pH. The experiment was conducted by the same method above except DAPI staining.

Intercellular drug release study of DTIG was investigated as the similar way. The cells of DTIG+laser group incubated with DTIG for 2 h were irradiated at the condition of 808 nm laser and 1.6 W cm^{-2} for 5 min and then incubated for another 0.5 h and 2 h respectively.

According to pre-selected intervals, the cells were fixed by 4% paraformaldehyde and then observed by CLSM.

The lysosome escape behaviors were also observed by CLSM. After the MCF7 cells were attached for 12 h, the old medium was replaced with fresh medium containing DTIG (10 μg mL^{-1} DOX) and further incubated for 1 h or 2 h. Next, the lysosomes were stained with Lyso-Tracker (Thermo Fisher, USA) for 0.5 h. Meanwhile, nuclei were stained with DAPI. Subsequently, the dye was replaced by fresh medium for observation.

Cytotoxicity assay. CCK-8 assay was used to investigate the cytotoxicity of DTIG. MCF7 cells (5×10^3 per well) were seeded in 96 well plate at 37℃ incubator overnight. Then, DOX, ICG, DOX+ICG and DTIG were added. For laser group, the cells were incubated with different formulations for 1 h and then irradiated at the condition of 808 nm laser and 1.6 W cm^{-2} for 5 min. After incubation for another 23 h, CCK-8 was added. The OD values were evaluated at 450 nm using an enzyme-labeled instrument (Bio-Tek, America).

***In vivo* bio-distribution assay.** DTIG were intravenously injected into MCF7 tumor-bearing nude mice with a tumor volume of 600 mm^3 at a dose of 50 μg kg^{-1} (ICG), and their bio-distribution were observed (n = 3) at 6 h, 24 h and 48 h by *in vivo* imaging system (Maestro *In-vivo* Image System, USA). The mice were sacrificed after *in vivo* imaging. The main organs and tumor tissues were collected for *in vitro* imaging.

***In vivo* pharmacokinetic study.** SD rats were injected intravenously with free DOX or DTIG (DOX was 6 mg kg^{-1}). 500 μL blood sample was collected at predetermined time points and centrifuged for 10 min (5000 rpm). After being extracted from the plasma, DOX fluorescence in the supernatant was measured with the excitation wavelength at 488 nm

and emission wavelength at 585 nm (Shimadzu, Japan).The pharmacokinetic parameters were calculated using a two-compartmental model by Phoenix® WinNonlin® 6.4.

***In vivo* anti-cancer therapy.** After the tumor volume reached 70-100 mm^3, 25 mice were randomly divided into 5 different groups. On the 1st and 3st day, mice were intravenously injected with DTIG+laser (DOX dose of 2.5 mg kg^{-1}), free DOX (DOX dose of 2.5 mg kg^{-1}), ICG+laser (ICG dose of 3.75 mg kg^{-1}), DOX+ICG+laser (DOX dose of 2.5 mg kg^{-1}) and 5% glucose (negative control group). For the laser treatment groups, the tumors of mice were irradiated by the 808 nm laser at 1 W cm^{-2} for 5 min. At last, organs and solid tumors were collected for hematoxylin and eosin (H&E), TUNEL and Ki67 examination.

1. Supplementary Figures and Tables

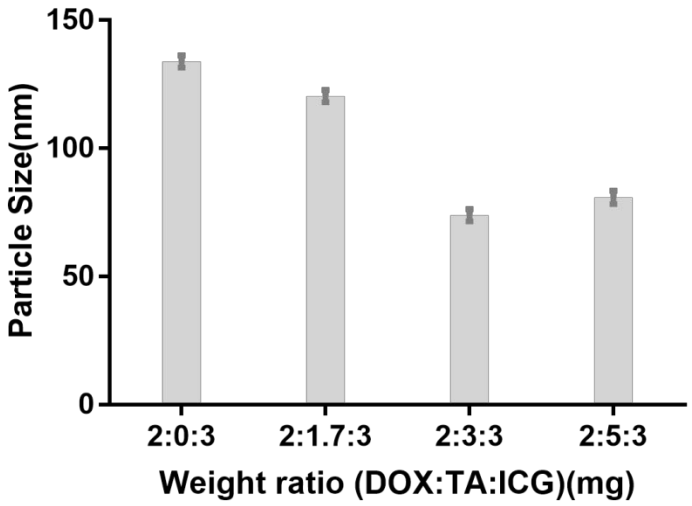

Figure S1. The particle size of DTIG at different weight ratios of DOX, TA and ICG (n=3).

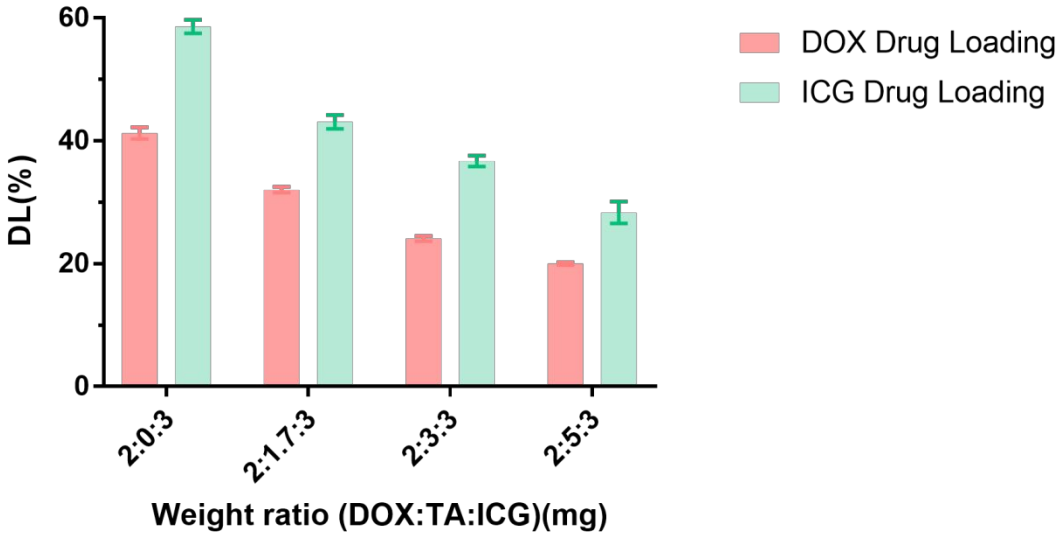

Figure S2. The drug loading (DL) of DTIG at different weight ratios of DOX, TA and ICG (n=3).

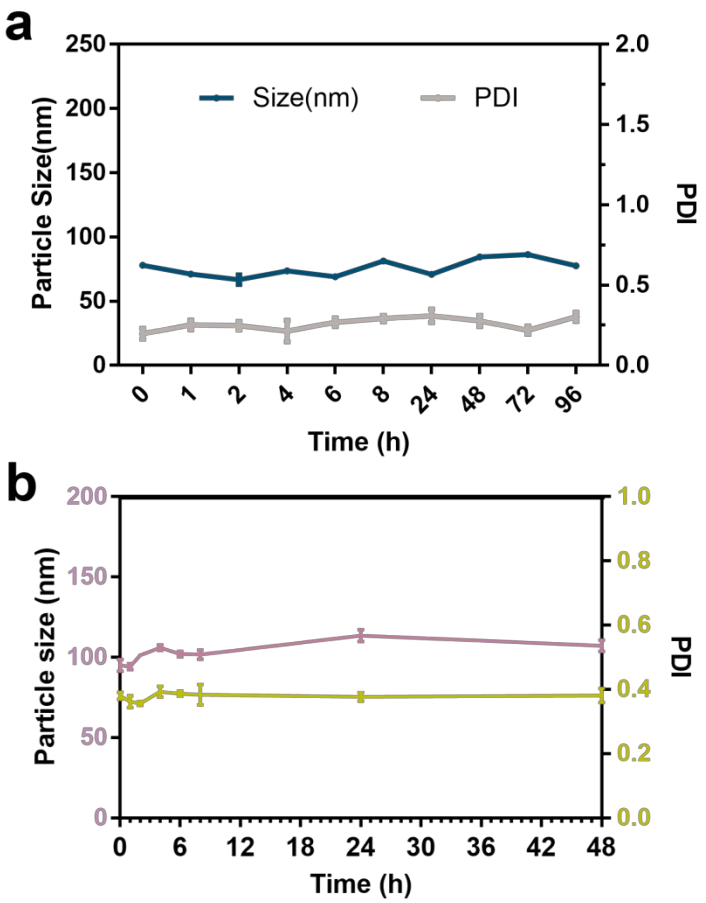

Figure S3. The stability of DTIG. (a)The particle size of DTIG solution within 96 h stored at 4 °C. (b) The particle size of DTIG in serum within 48 h.

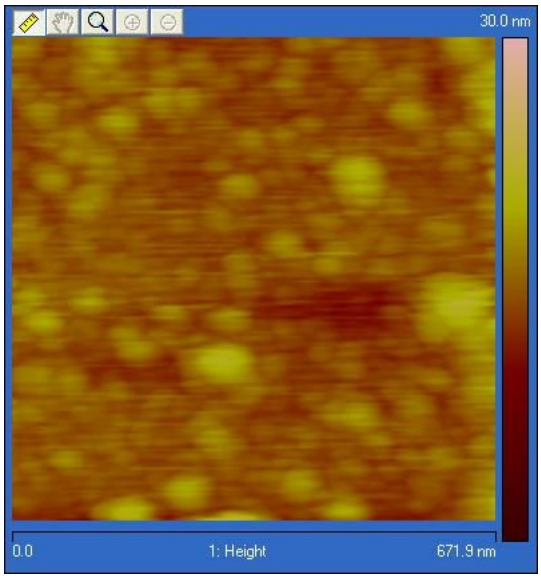

Figure S4. The AFM image of DTIG.

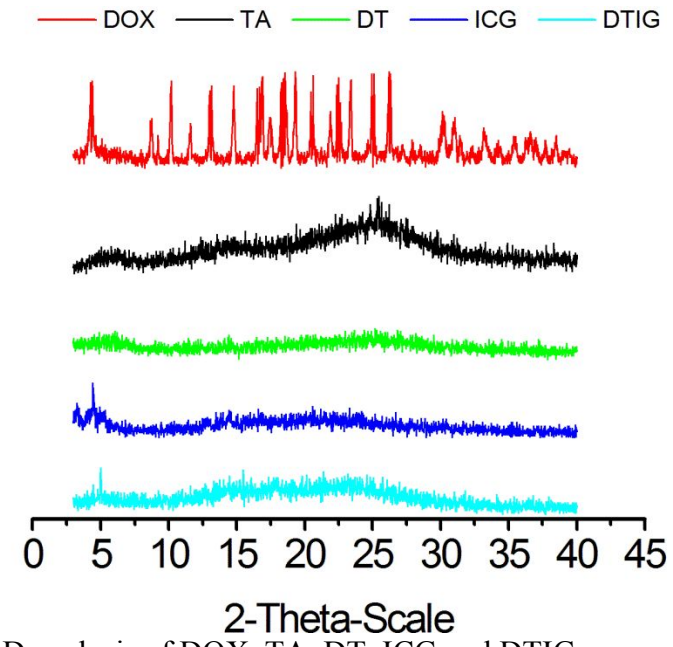

Figure S5. The XRD analysis of DOX, TA, DT, ICG and DTIG.

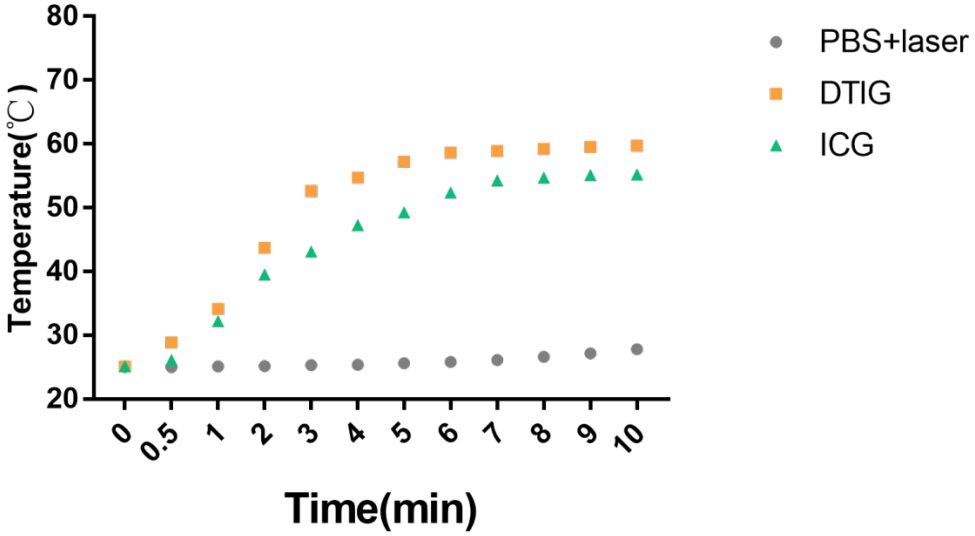

Figure S6. The temperature elevation of DTIG as a function of irradiation time.

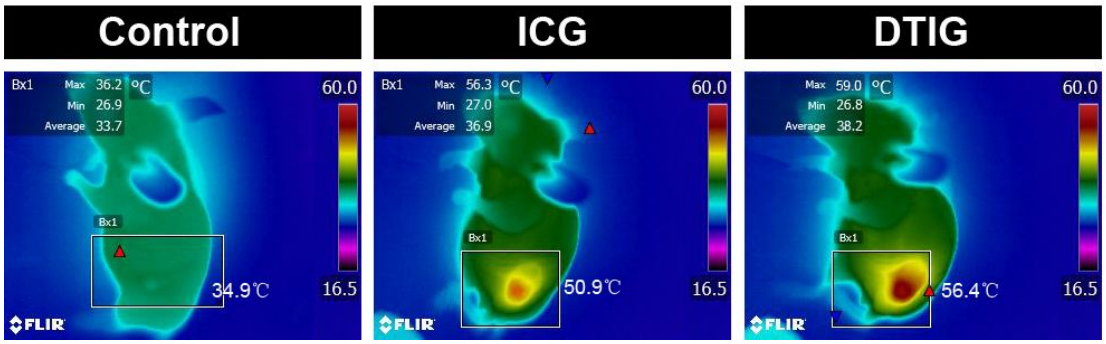

Figure S7. Infrared thermographic maps of mice injected with PBS, ICG and DTIG were measured at 5 min after laser irradiation.

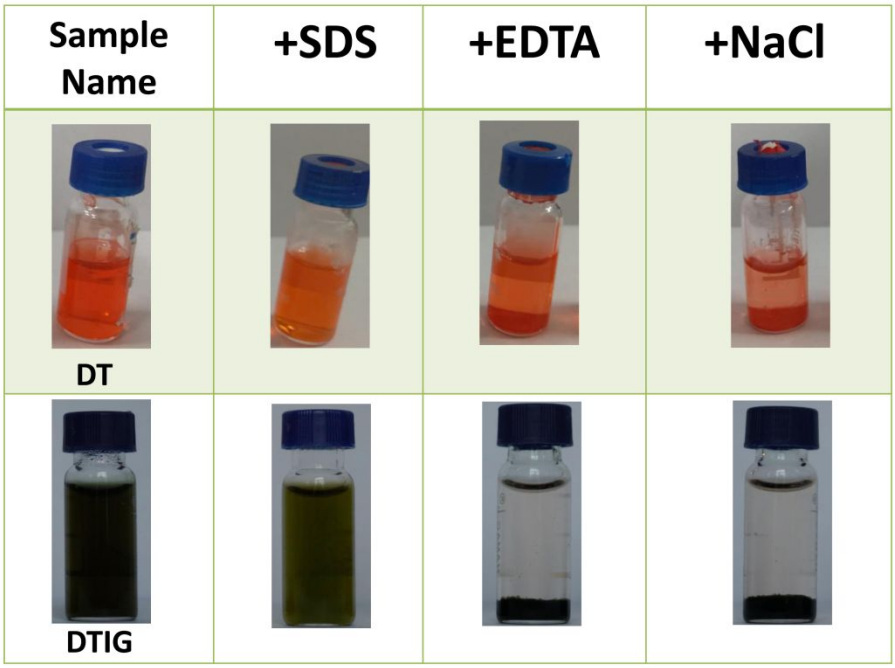

Figure S8. DTIG dissociation by NaCl, EDTA and SDS.

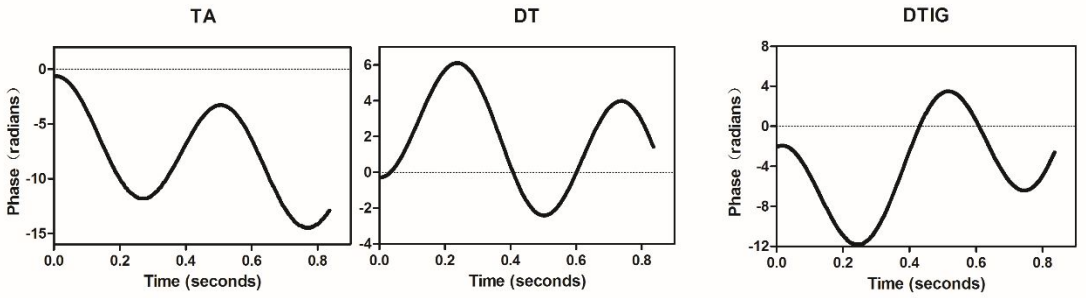

Figure S9. The zeta potential of TA, DT and DTIG.

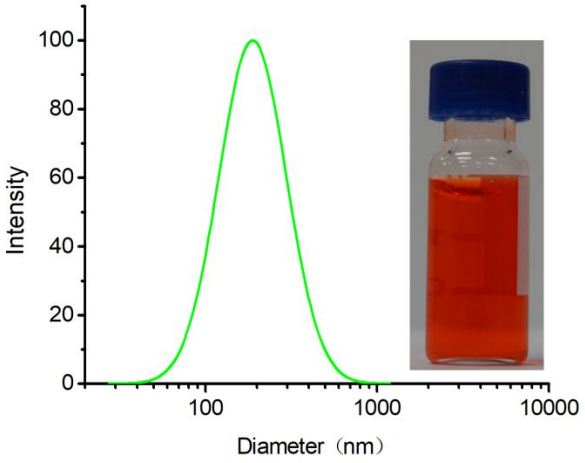

Figure S10. The particle size of DT. Insert was the image of DT solution.

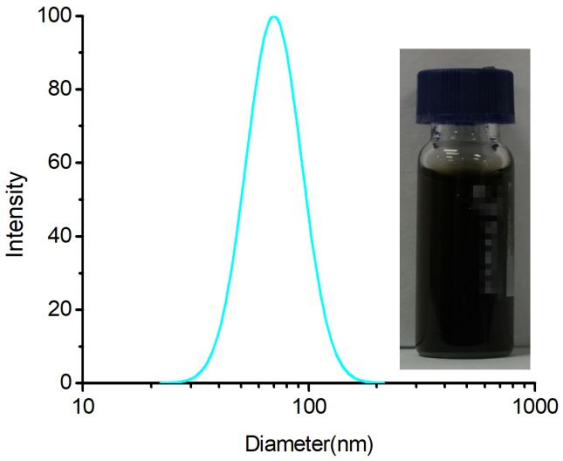

Figure S11. The particle size of DTIG. Insert was the image of DTIG solution.(Mosaic patterns are used to obscure trademarks.)

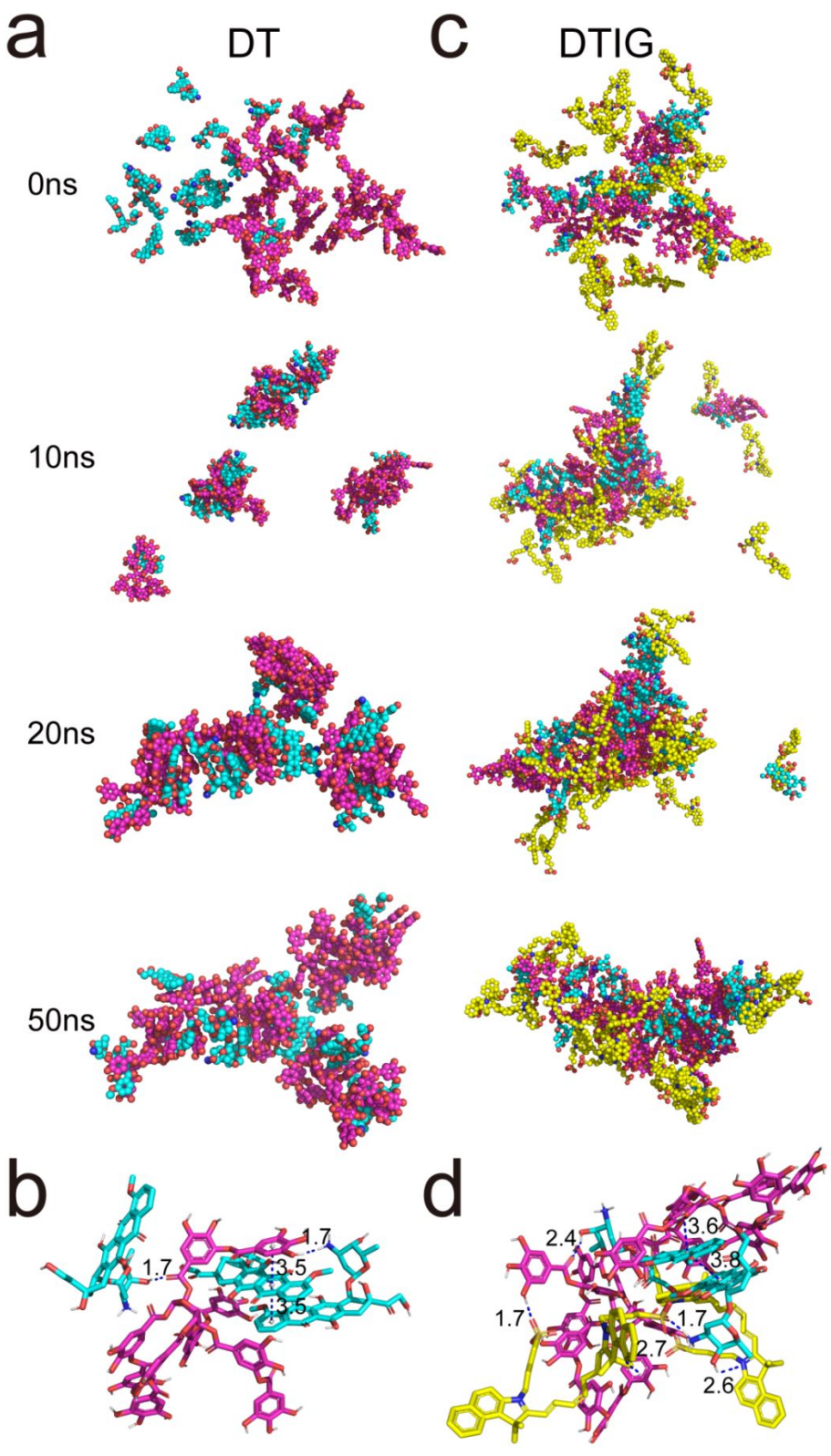
a
DT
c
DTIG
0ns
10ns
20ns
50ns
b
1.7
1.7
3.5
3.5
d
2.4
3.6
3.8
1.7
1.7
2.7
2.6

Figure S12. (a) The assembly of molecules DOX (cyan) and TA (purple). The structure image of DT shown in Figure 1i was the structure diagram of DT at 50ns. (b) Interactions between molecules DOX and TA. π-π interactions and salt bridge interactions between molecules are represented by blue line. The distances between the two neighbouring molecules were around 1.7-3.5 Å. (c) The assembly of molecules DOX (cyan), TA (purple) and ICG (yellow). The structure image of DTIG shown in Figure 1i was the structure diagram of DTIG at 50ns. (d) The interaction between representative molecules. DOX, TA and ICG are colored by cyan, purple and yellow respectively. π-π interactions and salt bridge interactions between molecules are represented by blue line. The distances between each two neighbouring molecules were around 1.7- 3.8 Å. This diagram was also shown in Figure 1i.

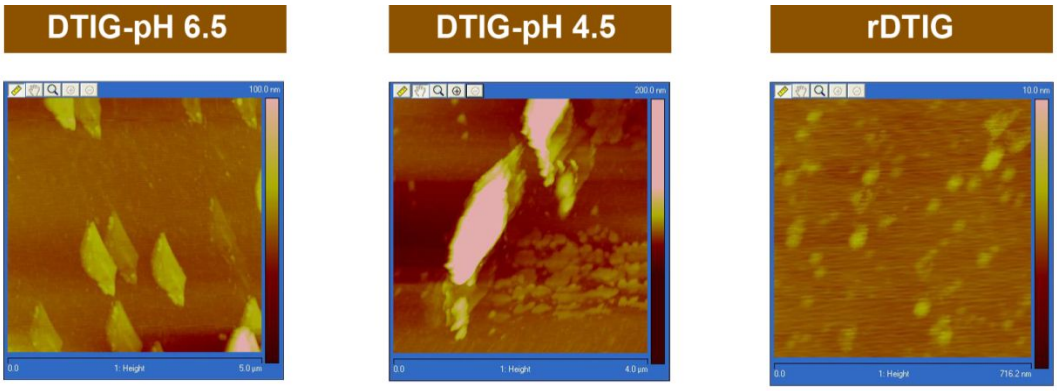

Figure S13. The AFM images of DTIG-pH6.5, DTIG-pH 4.5 and rDTIG.

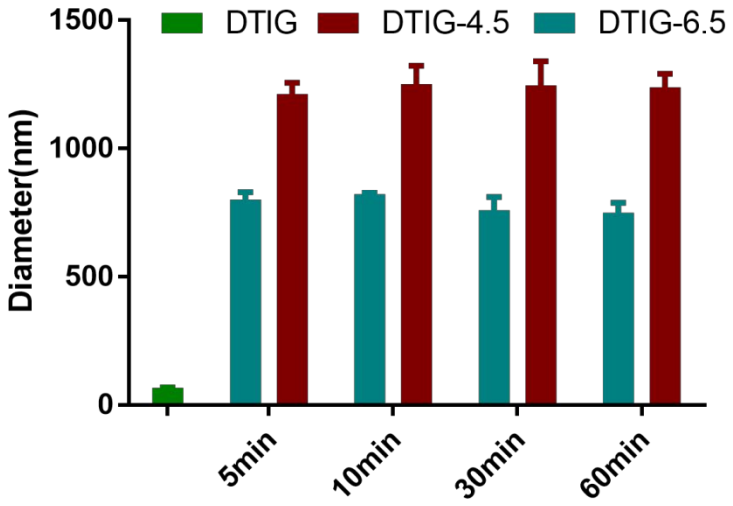

Figure S14. The particle size changes of DTIG-4.5 and DTIG-6.5 with time.

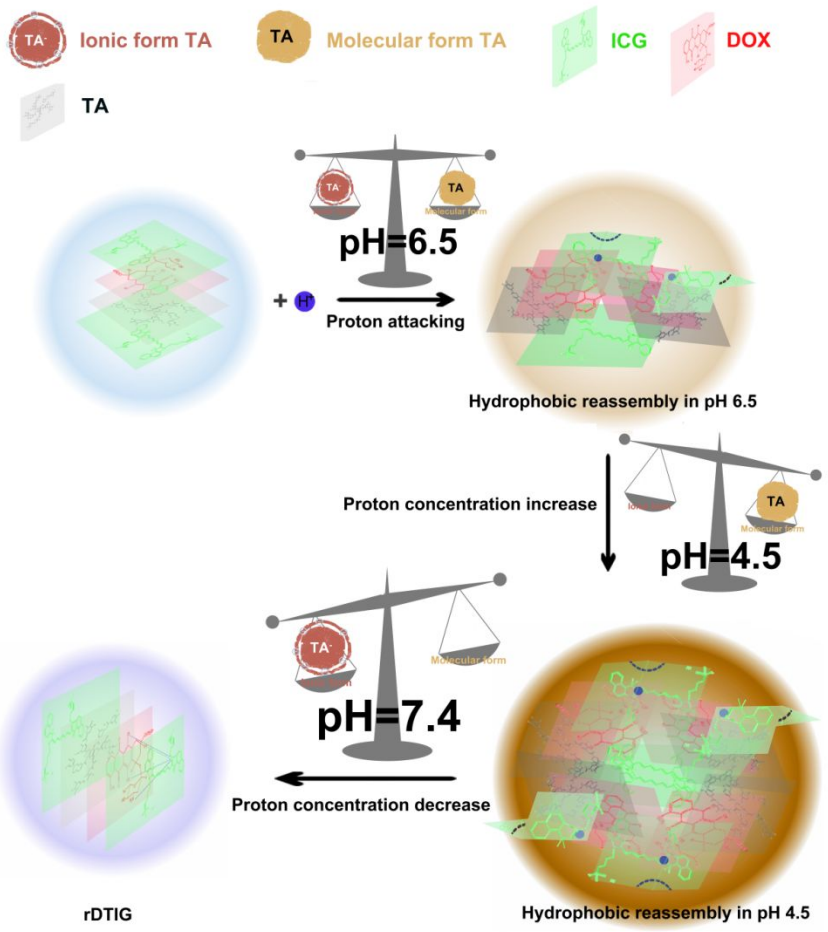

Figure S15. The proton-triggered transition mechanisms of DTIG.

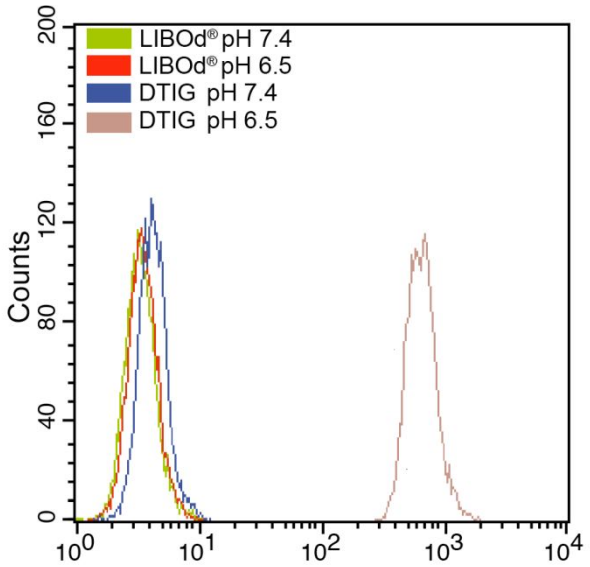

Figure S16. The Flow Cytometric Analysis. The MCF7 cell uptake amount of LIBOd® and DTIG in pH 7.4 and pH 6.5.

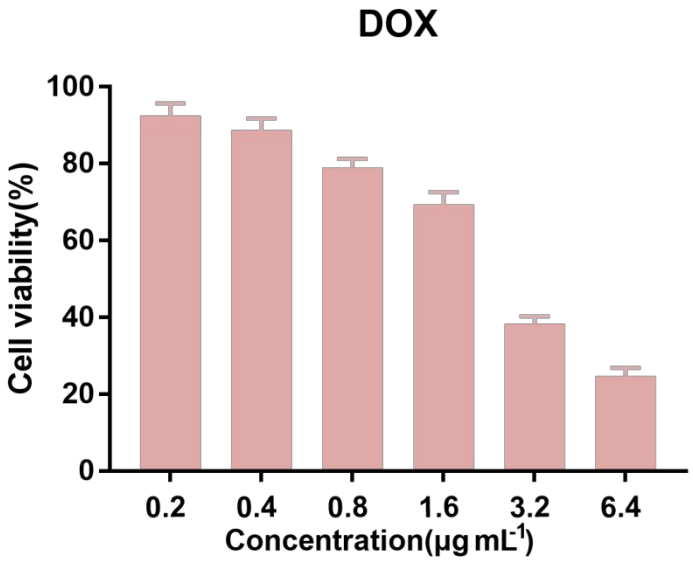

Figure S17. *In vitro* cytotoxicity of DOX against MCF7 cells for 24 h.

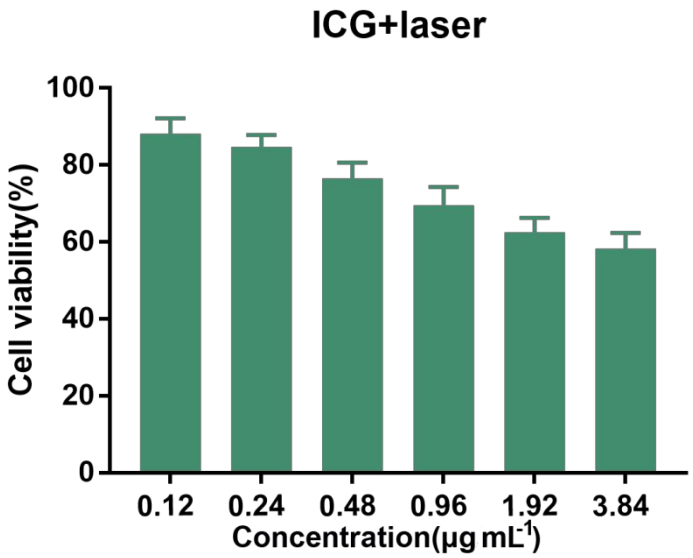

Figure S18. *In vitro* cytotoxicity of ICG +laser against MCF7 cells for 24 h.

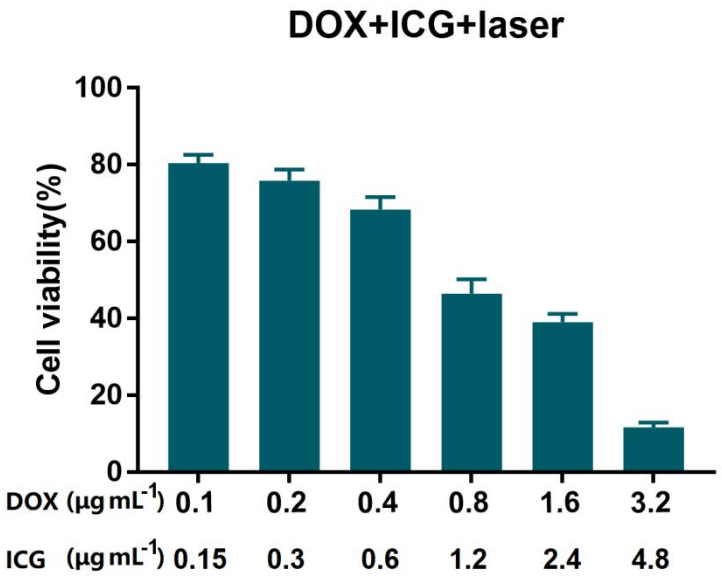

Figure S19. *In vitro* cytotoxicity of DOX+ICG +laser against MCF7 cells for 24 h.

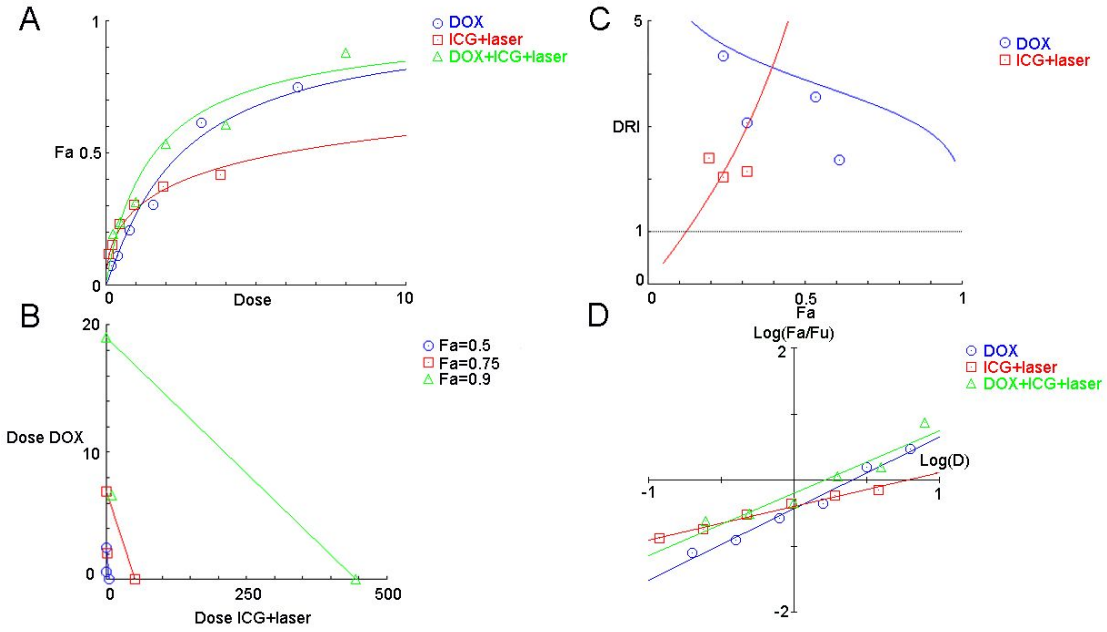

Figure S20. Results of CompuSyn analysis. (A) The dose-effect curve of combined use of DOX and ICG+laser. (B) Isobologram for combination therapy of DOX and ICG+laser. (C) DRI (Dose reduction index) plot for combination therapy of DOX and ICG+laser.(D) Median-effect plot for combination therapy of DOX and ICG+laser.

Table S1. The *in vivo* pharmacokinetics study of DTIG (n=3)

Parameter	DTIG	DOX
AUC(0-∞) (mg $L^{-1}h^{-1}$)	259.71±13.72**	111.787±6.85
$t_{1/2\alpha}$ (h)	0.843±0.39**	4.24±4.47
$t_{1/2\beta}$ (h)	33.20±2.89**	8.77±0.42
MRT(0-∞)(h)	33.49±4.84**	11.70±0.44
CL (L h^{-1} kg^{-1})	0.023±0.001	0.054±0.003
C_{max} (mg L^{-1})	8.67±0.55	8.08±0.05

**$p<0.01$ *vs.* DOX.

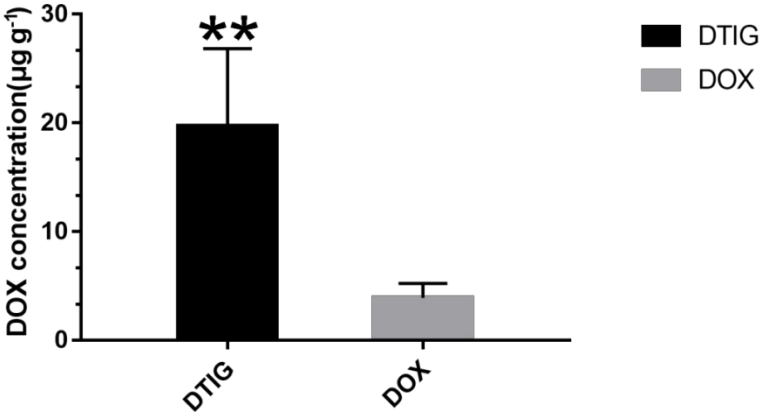

Figure S21. The concentration of DOX in tumor at 48 h post-injection (n=3).$^{**}p<0.01$ *vs.* DOX.

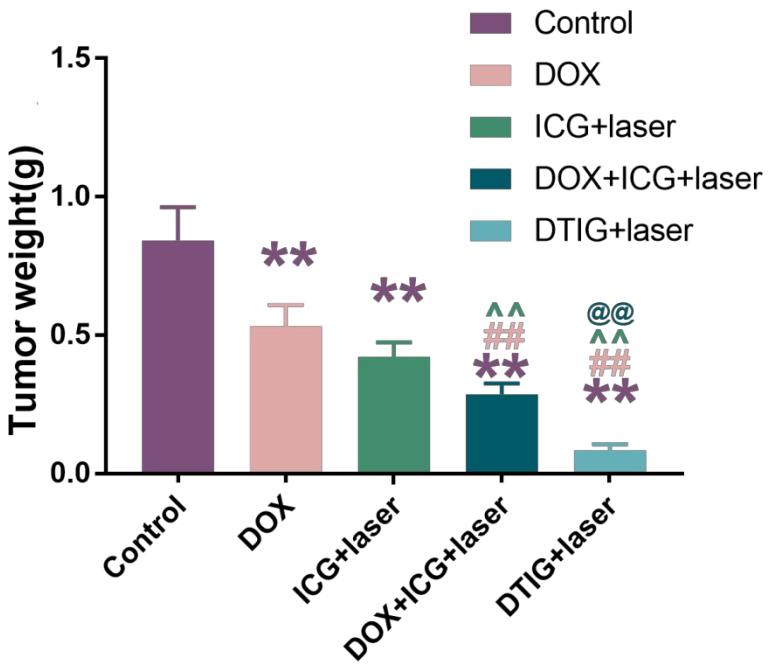

Figure S22. The tumor weights of MCF7-tumor bearing mice after treatment of different formulations (n = 5). $^{**}p < 0.01$ *vs.* control, $^{\#\#}p < 0.01$ vs. DOX, $^{\wedge\wedge}p < 0.01$ *vs.* ICG+laser, $^{@@}p < 0.01$ *vs.* DOX+ICG+laser.

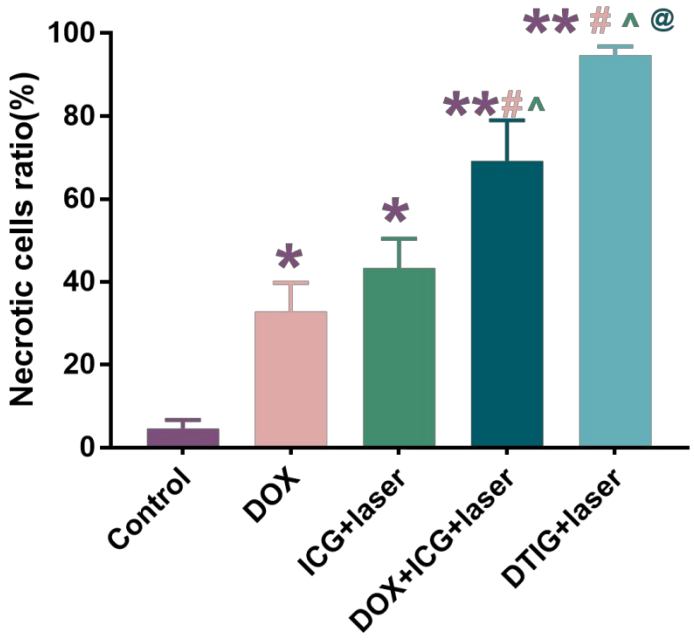

Figure S23. The necrotic cells percentage of tumor after treatment (n = 5). $^{*}p < 0.05$ *vs.* control, $^{**}p < 0.01$ *vs.* control, $^{\#}p < 0.05$ *vs.* DOX, $^{\wedge}p < 0.05$ *vs.* ICG+laser, $^{@}p < 0.05$ *vs.*DOX+ICG+laser.

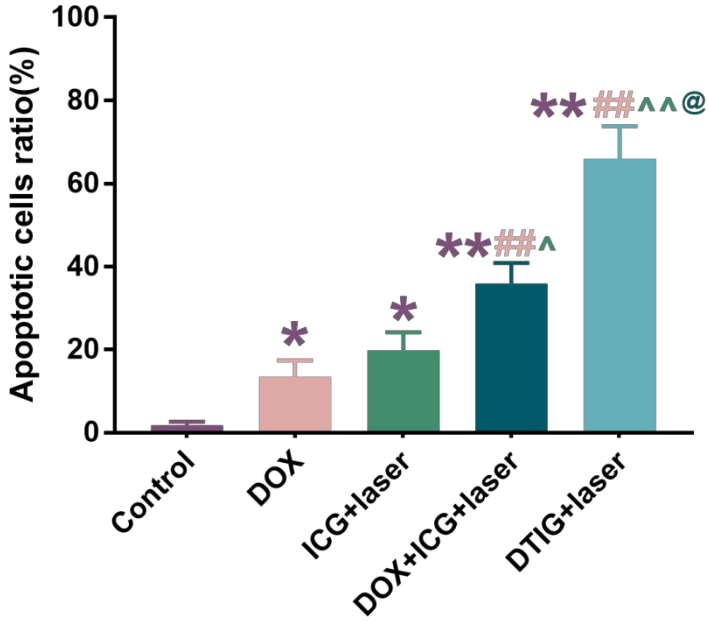

Figure S24. The apoptotic cells percentage of tumor after treatment (n = 5). $^{*}p < 0.05$ *vs.* control, $^{**}p < 0.01$ *vs.* control, $^{\#\#}p < 0.01$ *vs.* DOX, $^{\wedge}p < 0.05$ *vs.* ICG+laser, $^{\wedge\wedge}p < 0.01$ *vs.* ICG+laser, $^{@}p < 0.05$ *vs.*DOX+ICG+laser.

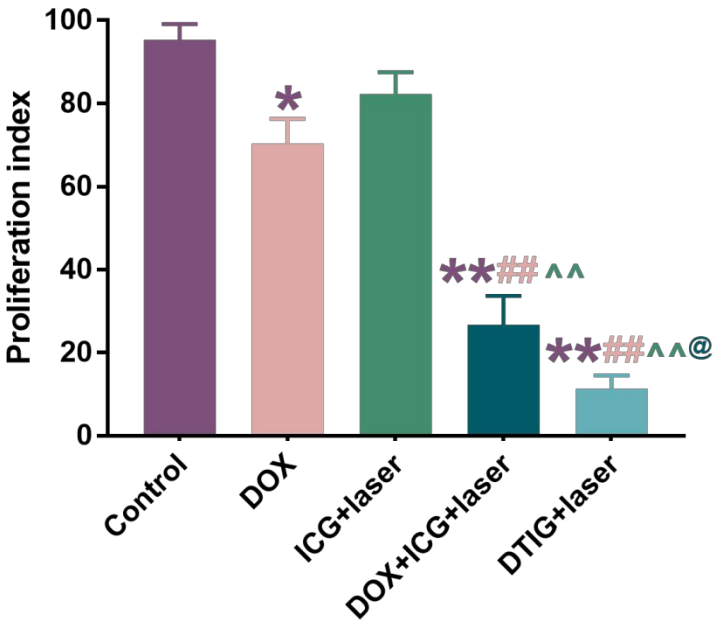

Figure S25. The proliferation index of tumor after treatment (n = 5). $^{*}p < 0.05$ *vs.* control, $^{\#\#}p < 0.01$ *vs.* DOX, $^{\wedge\wedge}p < 0.01$ *vs.* ICG+laser, $^{@}p < 0.05$ *vs.*DOX+ICG+laser.

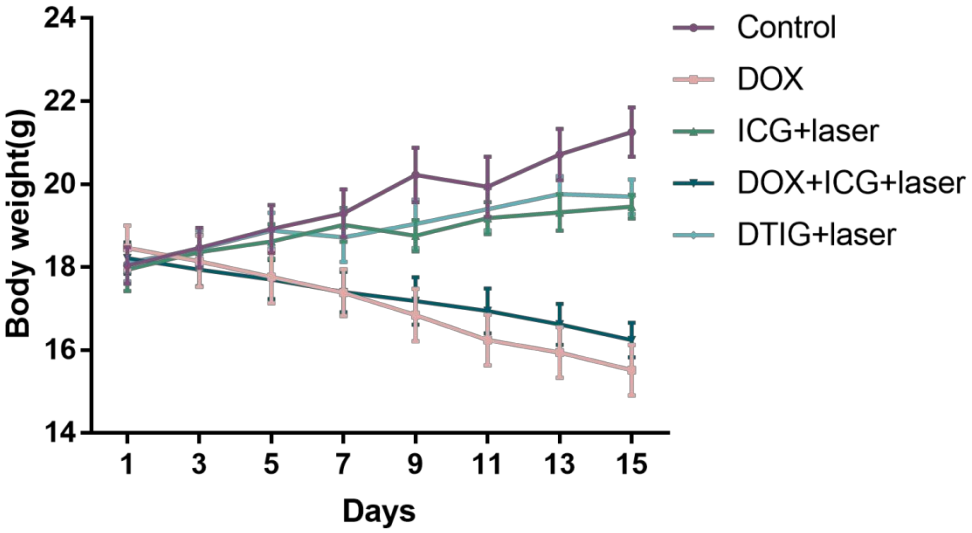

Figure S26. The body weight variation of MCF7 tumor-bearing mice during treatment (n = 5).

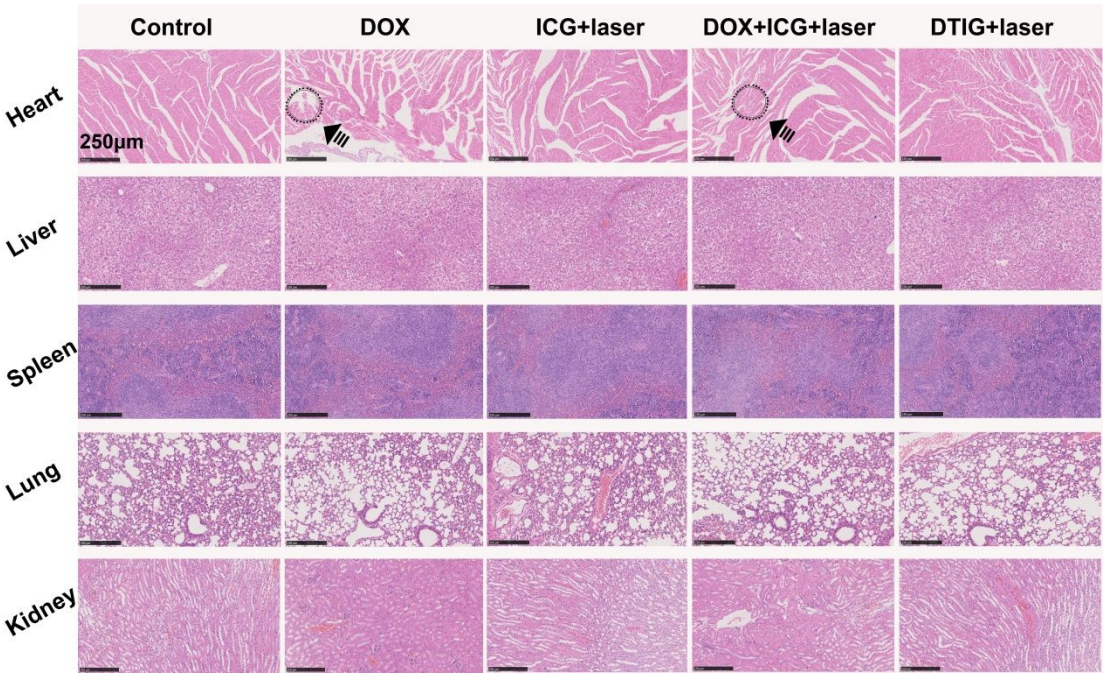

Figure S27. HE staining for pathological analysis of main organs (heart, liver, spleen, lung and kidney) of the mice bearing MCF7 tumors after treatments with different formulations. The circle areas indicated obvious pathological changes for potential tissue injury. Scale bars: 250 μm.

References

1. Gaussian 09, R. A., M. J. Frisch, G. W. Trucks, H. B. Schlegel, G. E. Scuseria, M. A. Robb, J. R. Cheeseman, G. Scalmani, V. Barone, G. A. Petersson, H. Nakatsuji, X. Li, M. Caricato, A. Marenich, J. Bloino, B. G. Janesko, R. Gomperts, B. Mennucci, H. P. Hratchian, J. V. Ortiz, A. F. Izmaylov, J. L. Sonnenberg, D. Williams-Young, F. Ding, F. Lipparini, F. Egidi, J. Goings, B. Peng, A. Petrone, T. Henderson, D. Ranasinghe, V. G. Zakrzewski, J. Gao, N. Rega, G. Zheng, W. Liang, M. Hada, M. Ehara, K. Toyota, R. Fukuda, J. Hasegawa, M. Ishida, T. Nakajima, Y. Honda, O. Kitao, H. Nakai, T. Vreven, K. Throssell, J. A. Montgomery, Jr., J. E. Peralta, F. Ogliaro, M. Bearpark, J. J. Heyd, E. Brothers, K. N. Kudin, V. N. Staroverov, T. Keith, R. Kobayashi, J. Normand, K. Raghavachari, A. Rendell, J. C. Burant, S. S. Iyengar, J. Tomasi, M. Cossi, J. M. Millam, M. Klene, C. Adamo, R. Cammi, J. W. Ochterski, R. L. Martin, K. Morokuma, O. Farkas, J. B. Foresman, and D. J. Fox, Gaussian, Inc., Wallingford CT. **2016**.
2. Wang, J. M.; Cieplak, P.; Kollman, P. A. *J Comput Chem* **2000,** 21, (12), 1049-1074.
3. A., H. T. *J Comput Chem* **1996,** 17, (5‐6), 490-519.
4. Martinez, L.; Andrade, R.; Birgin, E. G.; Martinez, J. M. *J Comput Chem* **2009,** 30, (13), 2157-64.
5. Wang, L. P.; McKiernan, K. A.; Gomes, J.; Beauchamp, K. A.; Head-Gordon, T.; Rice, J. E.; Swope, W. C.; Martinez, T. J.; Pande, V. S. *J Phys Chem B* **2017,** 121, (16), 4023-4039.
6. Case, D. A.; Cheatham, T. E., 3rd; Darden, T.; Gohlke, H.; Luo, R.; Merz, K. M., Jr.; Onufriev, A.; Simmerling, C.; Wang, B.; Woods, R. J. *J Comput Chem* **2005,** 26, (16), 1668-88.
7. Wang, J.; Wolf, R. M.; Caldwell, J. W.; Kollman, P. A.; Case, D. A. *J Comput Chem* **2004,** 25, (9), 1157-74.
8. Liu, X.; Fagotto, F. *Sci. Signal.* **2011,** 4, (203), pl2.